ACS APPLIED MATERIALS & INTERFACES

Research Article

www.acsami.org

Self-Healing Textile: Enzyme Encapsulated Layer-by-Layer Structural Proteins

David Gaddes,[†] Huihun Jung,[‡] Abdon Pena-Francesch,[‡] Genevieve Dion,[#] Srinivas Tadigadapa,[§,∥] Walter J. Dressick,[*,&] and Melik C. Demirel[*,‡,∥,⊥]

[†]Department of Bioengineering, [‡]Department of Engineering Science and Mechanics, [§]Electrical Engineering Department, [∥]Materials Research Institute, and [⊥]Huck Institutes of Life Sciences, Pennsylvania State University, University Park, Pennsylvania 16802, United States

[#]Westphal College of Media Arts and Design, Shima Seiki Haute Tech Lab at ExCITe, Drexel University, Philadelphia, Pennsylvania 19104, United States

[&]U.S. Naval Research Laboratory, Code 6910, 4555 Overlook Avenue, S.W., Washington, D.C. 20375, United States

Supporting Information

ABSTRACT: Self-healing materials, which enable an autonomous repair response to damage, are highly desirable for the long-term reliability of woven or nonwoven textiles. Polyelectrolyte layer-by-layer (LbL) films are of considerable interest as self-healing coatings due to the mobility of the components comprising the film. In this work mechanically stable self-healing films were fabricated through construction of a polyelectrolyte LbL film containing squid ring teeth (SRT) proteins. SRTs are structural proteins with unique self-healing properties and high elastic modulus in both dry and wet conditions (>2 GPa) due to their semicrystalline architecture. We demonstrate LbL construction of multilayers containing native and recombinant SRT proteins capable of self-healing defects. Additionally, we show these films are capable of utilizing functional biomolecules by incorporating an enzyme into the SRT multilayer. Urease was chosen as a model enzyme of interest to test its activity via fluorescence assay. Successful construction of the SRT films demonstrates the use of mechanically stable self-healing coatings, which can incorporate biomolecules for more complex protective functionalities for advanced functional fabrics.

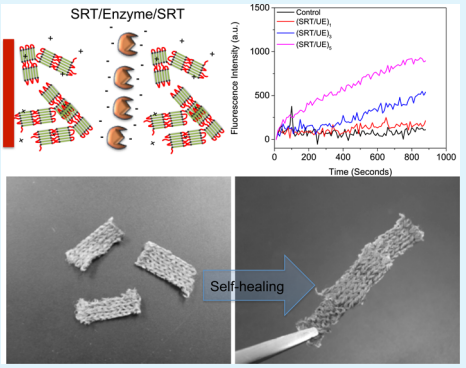

KEYWORDS: *squid protein, layer-by-layer, enzyme, textile, self-healing*

INTRODUCTION

Composite films exhibiting stimuli-triggered self-healing ability represent an increasingly important class of modern materials. For substrates prone to damage, such as certain biomedical implants,[1] metal surfaces,[2] or garments tailored for protection against chemical and biological warfare agents,[3,4] the ability to provide a coating capable of self-repairing microscopic or macroscopic defects[5] is highly desirable to ensure long-term reliability. Polyelectrolyte multilayers, prepared in a layer-by-layer (LbL) fashion by alternate treatments of a substrate with separate solutions of polycation and polyanion,[6] are especially attractive vehicles for fabricating self-repairing materials. Such films are conformally deposited onto a substrate surface under ambient conditions in safe solvents, such as water, at low cost using simple equipment amenable to scale-up.[7,8] In addition, film composition can be varied by inclusion of other charged species, such as nanoparticles,[9−12] macromolecules,[13] dyes,[14] and quantum dots,[15] among others,[16,17] that endow the film with multiple useful properties to enable new applications ranging from triggered chemical sensors[18,19] and drug delivery systems[20] to tunable catalysis.[21]

Polyelectrolyte multilayer films exhibiting self-healing properties generally comprise at least one weakly ionized polyelectrolyte component capable of diffusion within the deposited film during film deposition. Diffusion can be controlled by a variety of factors, such as polyelectrolyte molecular weight,[22] solution ionic strength,[13] and solution pH.[23] Diffusivity of a polyelectrolyte component within the film during film deposition leads to exponential film growth, in which large amounts polyelectrolytes are added to the film during each deposition cycle and very thick films (i.e., micrometers) containing intermixed, rather than stratified, polyelectrolyte components can be obtained. Whenever such a film is scratched or damaged, diffusion of polyelectrolyte from the film interior to the defect interface can lead to self-healing of the defect. The damaged film is typically exposed to water or dilute saline solution[24−27] to enhance the polyelectrolyte chain diffusion rate and thereby speed the healing process.

Received: May 2, 2016
Accepted: July 15, 2016

DOI: 10.1021/acsami.6b05232
ACS Appl. Mater. Interfaces XXXX, XXX, XXX−XXX

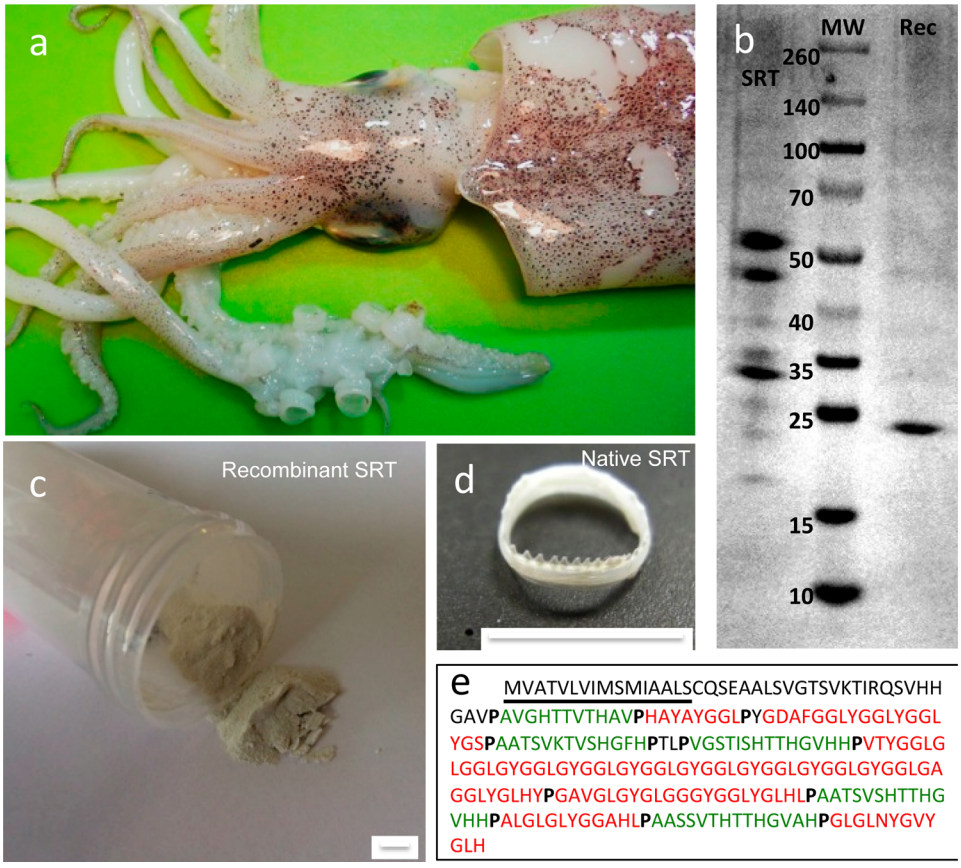

Figure 1. (a) Squid ring teeth are extracted from suction cups of *Loligo vulgaris* (European Common Squid). Recombinant protein sequence is identified using next generation sequencing approach and transcriptome assembly. The SDS-Page (b) shows sizes of native SRT complex and recombinant SRT proteins of 22 kDa. (c) Recombinant SRT (rSRT) protein (~1 g is shown) expressed in *E. coli* at a yield of 0.5 g/L (scale bar: 1 cm). (d) Native SRT protein complex has a ring structure and composed of several repetitive proteins ranging from 15 to 55 kDa (scale bar: 1 cm). (e) Amino acid sequence of rSRT reveals the segmented copolymer architecture, which is marked as red (Gly-rich amorphous region) or green (AVSHT-rich crystalline region), separated by proline residues (bold black). The first 20 amino acids (underlined) are the signal peptide.

Most examples of self-healing LbL polyelectrolyte multilayer films to date utilize branched polyethylenimine (b-PEI) and poly(acrylic acid) (PAA) as film components,[24−31] though other systems have also been reported.[32−35] Healing of defects having widths of tens of micrometers in b-PEI/PAA films can occur in as little as 5−30 min in the presence of water or dilute saline solutions[24,26,27] and 1−2 h in air atmosphere at 100% relative humidity.[28] Faster healing in water has been observed for films containing Ag[29] or graphene[30] nanoparticles, which are thought to enhance film water swelling and plasticization. Although these defect repair times are generally adequate for many applications, a key impediment to more widespread use of these films is their mechanical stability. For example, b-PEI/PAA films exhibit a tendency to crack when exposed to warm, dry conditions for extended periods, though such films again self-repair when subsequently exposed to water.[30] Nevertheless, cracking behavior subverts their ability to protect the underlying substrate. Polyelectrolyte multilayer film brittleness and cracking can be partially ameliorated via inclusion of nanoparticles[33] in the films and/or partial cross-linking[34] of the polyelectrolyte components, both of which toughen the film while preserving its self-healing properties. However, these approaches, though promising, do not currently provide an adequate solution.

Nature provides custom engineered materials in the form of structural proteins exhibiting a range of mechanical properties. In particular, we have been examining mechanical and related properties of squid ring teeth proteins (SRT) isolated from the suction cups of squid. These proteins are readily extracted and expressed in gram-scale quantities sufficient for examination as potential new materials. We have shown previously[36−39] that such proteins exhibit unique combinations of toughness and elasticity that persist in both their wet and dried states, rendering them interesting candidates for fabrication of self-healing multilayer films capable of resisting dry cracking. Here we demonstrate for the first time the self-healing and mechanical properties of multifunctional polyelectrolyte multilayer films based on SRTs with urease enzyme (UE) or polystyrenesulfonate (PSS) and their use as protective films on textile materials. We show that stable films can be reproducibly deposited on a textile substrate to form a composite that resists dry cracking, self-heals macroscopic textile tears in the presence of water, and maintains urease enzyme activity as a first step in utilizing SRTs for fabrication of more advanced multifunctional coating materials.

RESULTS AND DISCUSSION

Squid ring teeth (SRT) proteins constitute a unique class of high-performance semicrystalline structural proteins extracted from the suction cups of squid tentacles as shown in Figure 1a. SRT is a protein complex composed of several proteins with repetitive sequences similar to a segmented copolymer[38] that

DOI: 10.1021/acsami.6b05232
ACS Appl. Mater. Interfaces XXXX, XXX, XXX−XXX

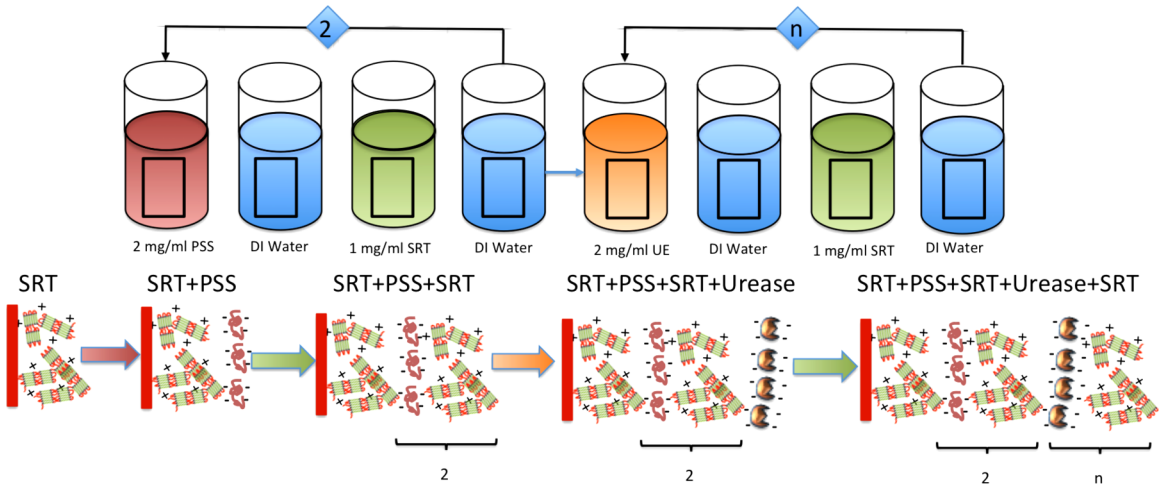

Figure 2. Fabrication of the multilayer structure on SRT-coated cotton substrate. (top) Dip-coating method to form (UE-SRT) multilayered structure. (bottom) Schematic of the multilayer structure at each dip-coating step is shown. PSS: polystyrenesulfonate; SRT: squid ring teeth protein; UE: urease.

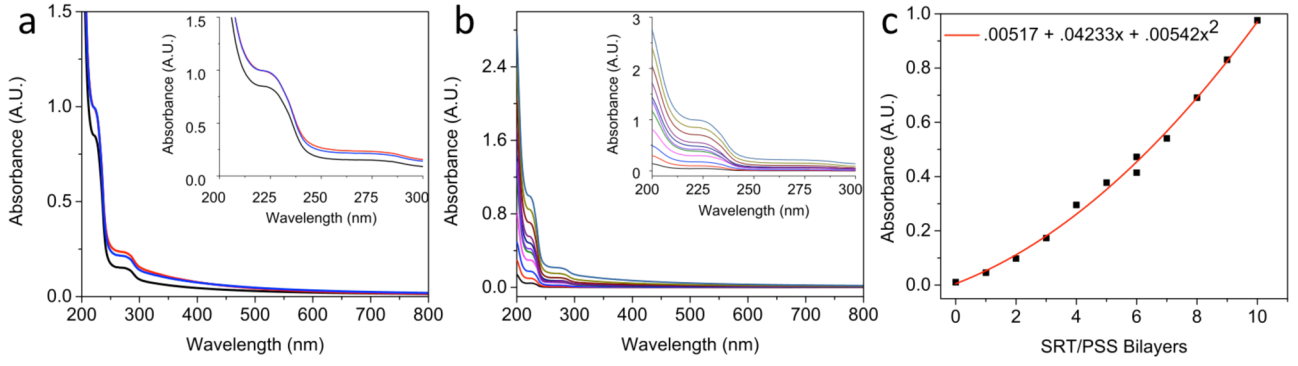

Figure 3. UV−vis characterization of multilayer structure and growth: (a) PSS contribution to UV−vis absorbance. The black line represents 9th SRT/PSS bilayer film, the red line the 10th SRT/PSS bilayer film, and the blue line 9.5th SRT/PSS bilayer film. (inset) Amplified far UV range. (b) UV−vis absorbance spectra of complete deposition of bilayers (i.e., 0−10th) of PSS-SRT. (inset) Expanded far UV range. (c) Absorbance of 0−10 PSS/SRT bilayers at 225 nm from the UV−vis data. Red line shows the parabolic fit to the absorbance data.

exhibits strong mechanical properties in both air and water (e.g., elastic modulus of 6−8 and 2−4 GPa, respectively).[36] Recombinant expression of SRT is of interest for scaled-up applications as the native SRT protein is inefficient to collect and requires the sacrifice of a squid. The protein gel electrophoresis results (Figure 1b) show the sizes of recombinant 22 kDa SRT protein (rSRT) expressed in *E. coli* at a yield of 0.5 g/L (Figure 1c) and native SRT protein complex from *Loligo vulgaris* (Figure 1d). The sequence of the recombinant protein is provided in Figure 1e. The soft amorphous regions, red colored regions, play an important role in self-healing while the β-sheet domain, green colored regions, give rise to the strong mechanical properties. The self-healing capability of SRT results from the soft amorphous regions of the protein enabling a supramolecular self-assembly capability to form a strong adhesive bond in the presence of water and reversible glass-to-rubber transition. In this work both native and recombinant expressed squid ring teeth proteins are used to construct self-healing layer-by-layer (LbL) films.

For the proof of concept, urease enzyme is chosen for LbL studies. Urea forms as proteins breakdown in the body. Specifically blood urea nitrogen is commonly monitored to diagnose liver and kidney function.[40] Moreover, urease is frequently used in biosensors[41] to monitor kidney function.[19,42] Urease immobilized using a LbL technique can retain >80% activity in solution at 25 °C.[43] When developing biosensors incorporating enzyme containing LbL films, the catalytic activity of the film should be maximized. Sakr et al.[44] showed that diffusion limitation of analytes into the enzyme containing LbL film could decrease return on enzymatic activity. Therefore, the number of layers in functional LbL films expressing enzymatic activity does have an upper bound due to analyte diffusion limitation (e.g., 5−7 bilayers).

Polyelectrolyte multilayers are formed using a dip coating method illustrated in Figure 2. First, LbL thin films were formed with a polyelectrolyte and SRT, and then complex films with an enzyme and SRT were prepared. The former contains SRT and polystyrenesulfonate (PSS) and serve to quantify the film growth dynamics. The latter contains SRT and urease (UE), which demonstrates that SRT can form a self-healing film with a functional biomolecule. The PSS solution used contains 1 M sodium chloride to shield repulsive intermolecular electrostatic interactions. To this initial layer of PSS a layer of SRT is adsorbed to form the first bilayer. For the UE + SRT bilayers, a cushion bilayer of PSS−SRT is formed to ensure adequate separation of silicon dioxide and urease to preserve

DOI: 10.1021/acsami.6b05232
ACS Appl. Mater. Interfaces XXXX, XXX, XXX−XXX

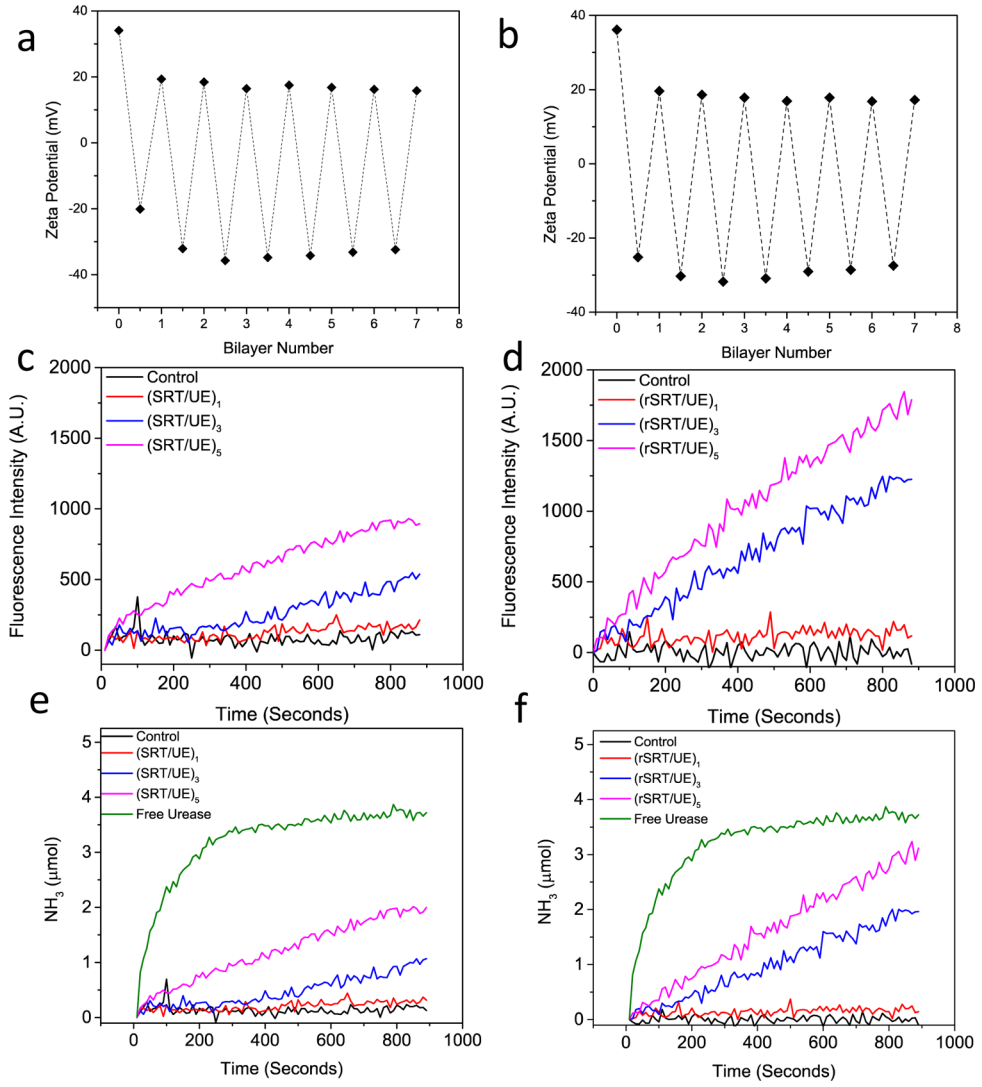

Figure 4. Multilayer adsorption and enzymatic activity: multilayer deposition monitored by ζ-potential with (a) native and (b) recombinant SRT proteins and urease (UE). Note that the first two bilayers are of PSS−SRT, followed by five bilayers of UE−SRT. Enzymatic activity of urease in (c) native and (d) recombinant SRT-LbL architecture measured by a colorimetric assay using a fluorescent pH-sensitive dye. Enzymatic activity of urease is compared with the free urease for (e) native and (f) recombinant SRT-LbL architecture. Fluorescence intensity is converted to NH_3 concentration using the Hendersen−Hasselbach equation.

urease activity. Following fabrication of the base bilayers the desired number of UE + SRT bilayers is formed.

Construction of a PSS/SRT self-healing film was characterized using UV−vis spectroscopy as proof of SRT incorporation into a multilayer as well as to observe the growth dynamics of the multilayer. PSS and SRT were alternatively adsorbed on quartz substrates coated with *N*-(2-aminoethyl)-3-aminopropyltrimethoxysilane (EDA)[45] until 10 bilayers of PSS/SRT were formed. The UV−vis spectra of consecutive bilayers are displayed in Figures 3a and 3b for bilayers of 9−10 and 0−10, respectively. In Figure 3a, the spectrum of a Q-EDA/PSS/$(SRT/PSS)_9$ film terminated by a PSS layer (i.e., 9 SRT/PSS bilayers; black spectrum) is shown, together with the spectra of a film obtained by addition of the next SRT layer (i.e., Q-EDA/PSS/$(SRT/PSS)_9$/SRT; 9.5 SRT/PSS bilayers; blue spectrum) and next PSS layer (i.e., Q-EDA/PSS/$(SRT/PSS)_{10}$; 10 SRT/PSS bilayers; red spectrum). The blue and red lines are nearly identical, which demonstrates that a small amount of PSS is depositing and SRT predominantly contributes to the UV−vis adsorption. The increase in absorbance at 225 nm, where PSS absorbs light, after deposition of a PSS layer is typically less than or equal to the uncertainty of our absorbance measurement (i.e., 0.0004 units), suggesting that adsorption of as little as a monolayer of PSS is sufficient to continue multilayer growth. The far-UV region of SRT-PSS bilayers is amplified in Figure 3a and 3b insets. The monotonic increase of absorbance with increasing bilayers in Figure 3b confirms SRT and PSS are capable of forming a multilayered structure. The film absorbance at 225 nm plotted against the number of SRT/PSS bilayers is shown in Figure 3c. The multilayer grows in a parabolic manner. This is consistent with the typical growth regime of polyion multilayers, in which films grow parabolically prior to a transition to a linear growth regime after some number of bilayers.[46]

The construction of a complex multilayer film containing urease (UE) enzyme was monitored by the zeta (ζ)-potential of the films deposited onto glass particles. Multilayers containing UE were constructed using both native and recombinant SRT. Microelectrophoresis was used to determine the ζ-potential of the outermost layer alternates for UE/SRT or UE/rSRT.

DOI: 10.1021/acsami.6b05232
ACS Appl. Mater. Interfaces XXXX, XXX, XXX−XXX

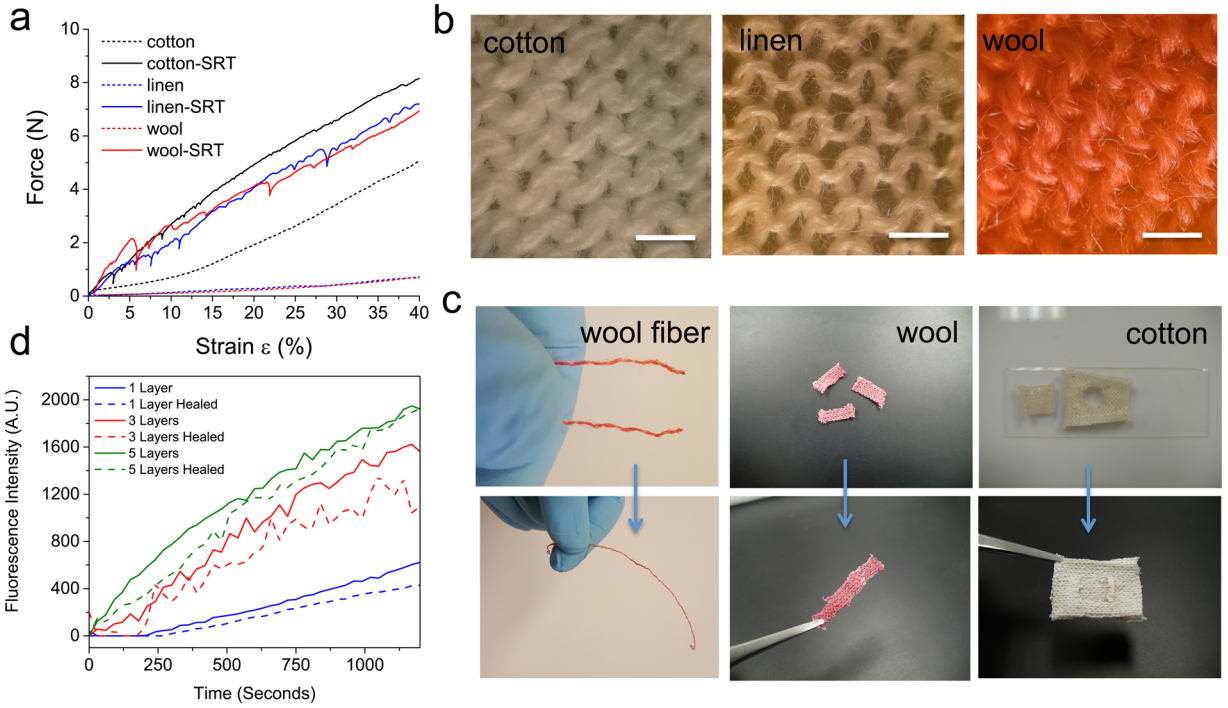

Figure 5. (a) Mechanical analysis of SRT-coated cotton, linen, and wool fabrics are shown. Note that the *y*-axis is shown in force units (N) to provide an accurate response for varying textile morphology shown in (b). In all three cases, SRT-coated textile is stronger compared to bare textile. (c) Fluorescence data for the coated cotton textile reveal that the enzymatic activity of urease in SRT-LbL architecture is preserved before and after healing. (d) SRT-coated fabric can self-heal within seconds (see also Supporting Information movie).

Successful alternating deposition of these polyelectrolytes will result in a charge inversion on the surface ζ-potential each time a new layer is deposited. The multilayers were constructed on *N*-(2-aminoethyl)-3-aminopropyltrimethoxysilane-coated controlled pore glass (EDA-CPG) particles. The ζ-potential at each stage of deposition is shown in Figures 4a and 4b for UE/SRT and UE/rSRT films, respectively. As discussed earlier, prior to construction of the UE mutlilayers, two bilayers of PSS/SRT are deposited onto the EDA-CPG as cushion layer, which act as a barrier between the enzyme and the glass.

Following fabrication of the PSS/SRT base layers, five bilayers of SRT/UE are coated on the glass particles. As displayed in Figures 4a and 4b, the ζ-potential of the particles changed from +15−20 mV for SRT (and for rSRT, respectively) to −30−35 mV for UE. This switching in the surface charge polarity indicates successful self-assembly of the UE/SRT or UE/rSRT multilayers onto the EDA-CPG particles. The stable ζ-potential indicates no aggregation occurs during construction of UE/SRT multilayers, as aggregation decreases the mobility of the colloid particles, resulting in a decrease in ζ-potential. The inversion of surface charge polarity is necessary for the subsequent LbL assembly of oppositely charged polyelectrolyte on the coated colloidal particles. Comparison of Figures 4a and 4b indicates that identical deposition of the native and recombinant SRT occurs during film deposition with urease, leading to reproducibly deposited and uniform films, as expected.

The LbL architecture also provides a platform to stabilize the immobilized enzyme,[3] opening new possibilities for complex self-healing films. The activity of the urease was investigated using a fluorescence assay to demonstrate the functionality of incorporated enzyme in the LbL film. Urease catalyzes the hydrolysis of the molecule urea into two ammonium species, raising the pH of the solution. Therefore, a pH-sensitive fluorescent dye was used to investigate the enzymatic activity of the UE/SRT multilayers.[19] Initially, the dye was calibrated to ensure the experiments were operated in a pH range in which the change in pH linearly affected the fluorescence intensity of the dye. UE/SRT or UE/rSRT multilayers were constructed on a 4 cm × 4 cm EDA coated glass slide with 2 base bilayers of PSS/SRT to prevent inhibition of enzymatic activity. Furthermore, we constructed 1, 3, and 5 bilayers of UE/SRT or UE/rSRT on top of the PSS/SRT to demonstrate the increased activity of UE as multilayers are deposited. The data presented in Figure 4c demonstrate that as the number of urease containing bilayers is increased the rate of hydrolysis of urea is increased for native SRT layers. Similarly, the data in Figure 4d demonstrate the same principle with recombinantly expressed SRT and urease bilayers. For both films, the enzyme activity is compared to free enzyme in solution in Figures 4e and 4f.

To illustrate the SRT films' ability to self-heal large defects while maintaining enzymatic activity, we coated knitted textiles made of wool, cotton, and linen fibers with the multilayer film. Mechanical properties of the SRT coated and bare textiles (Figure 5a) were studied by dynamical mechanical analysis (DMA). Uncoated samples present a smother but weaker response in mechanical analysis compared to SRT coated samples due redistribution of forces and composite effects in knitted fabrics. Optical images of knitted morphology of three samples are shown in Figure 5b. Furthermore, we demonstrate that the enzymatic activity of the SRT-coated wool fibers are retained after the self-healing process. Using the fluorescent assay described previously, we analyzed the enzyme kinetics before and after self-healing. The data displayed in Figure 5c demonstrate little enzymatic activity is lost between cutting and

DOI: 10.1021/acsami.6b05232
ACS Appl. Mater. Interfaces XXXX, XXX, XXX−XXX

repairing the coated cloth. The SRT-coated cotton fiber and textile sample were cut into two and three pieces, respectively, and repaired by applying pressure and warm water as seen in the Figure 5d (see also Supporting Information movie). Similarly, a patch is repaired in an SRT-coated wool sample as shown in Figure 5d (see Supporting Information movie). A slight reduction in the fluorescence activity after the healing process is observed due to loss of substrate (and hence LbL layers with the enzyme) in the cutting process. The underlying mechanism for self-healing is the ability of the SRT protein to deform and soften in water above its glass transition temperature, while maintaining the hydrogen bonds reversibly in the amorphous region.[39]

CONCLUSION

SRT is a protein-based segmented copolymer that exhibits a self-healing property due to its molecular architecture. We have demonstrated enzyme encapsulation in SRT−PSS base layers on glass surfaces as well as knitted textiles. Our results clearly demonstrate that the LbL method is applicable to deposition of SRT-containing multilayer films with increased mechanical properties and self-healing characteristics onto conventional textiles (i.e., cotton, linen, and wool). Moreover, we have demonstrated a composite enzyme-SRT self-healing film that retains enzyme activity even after repairing large defects. Such complex films may enable a coating for multifunctional applications in programs such as Second Skin,[47] where advanced fabrics protect wearers from chemical and biological warfare agents by restricting the pores of the clothing to block out harmful agents.[47] A mechanically stable, self-healing film containing enzymes such as organophosphorus hydrolase,[3] which neutralize chemical agents, would prove critical to such an application to actively neutralize these threats as well as ensure no micro- or macroscale defects permit leaks.

SRTs hold great promise to provide a broad range of solutions for textile applications due to their ability to self-heal. Manipulating the protein network structure of SRT is a prerequisite to develop additional novel material properties emerging from the atomic scale that are retained in much larger product-scale for materials fabrication. Utilization of LbL technologies to prepare such films offers the advantages of low cost and versatile processing compatible with modern advanced textile manufacturing. Furthermore, biopolymers such as SRTs and silk proteins are environmentally superior alternatives to synthetic plastics, which will minimize waste and pollution. As the cost of production for industrial biotechnology products continues to fall, such self-healing and enzyme containing films become increasingly feasible and sustainable for large-scale productions.

METHODS AND MATERIALS

Expression of Recombinant SRT. A single colony of *E. coli* was inoculated and grown overnight in 250 mL of LB (Lysogeny broth) with ampicillin (100 μg/mL). The overnight culture was inoculated into an 80L fermenter containing LB/ampicillin (100 μg/mL). The culture was grown at 37 °C to an OD600 of 0.6 when IPTG (isopropyl β-D-1-thiogalactopyranoside) was added. The cells were then pelleted at 10 000 rpm for 15 min and washed twice with 20 mM Tris buffer pH 8. The cell pellet was then resuspended in 50 mL of lysis buffer (50 mM Tris pH 7.4, 200 mM NaCl, 1 mM PMSF (phenylmethylsulfonyl fluoride), 10 mg/mL lyzosyme, 0.1 mg/mL DNase I, and 2 mM EDTA) and lysed using a high-pressure homogenizer. The lysed cells were pelleted at 14 000 rpm for 1 h at 4 °C. The pellet was then washed twice with urea extraction buffer (100 mM Tris pH 7.4, 5 mM EDTA, 2 M urea, 2% (v/v) Triton X-100) and then twice with a wash buffer (100 mM Tris pH 7.4, 5 mM EDTA). After the washing step, the recombinant proteins were dried using a Freezezone 12 (Labconco, Kansas City, MO) freeze-dryer. Recombinant proteins of ∼90% purity were obtained in this manner and yields were estimated at ∼0.5 g/L.

Native SRT Collection. European common squids (*Loligo vulgaris*) were captured from the coast of Tarragona (Spain). Native SRT was removed from the tentacles while washing it with deionized (DI) water and ethanol mixture (70:30 ratio v/v) and kept in the ethanol/water solution overnight. The rings were pulverized in liquid nitrogen using a ceramic mortar and pestle after vacuum drying.

Layer-by-Layer Immobilization Protocol. A 2 mg PSS/mL 1 M NaCl/pH 3 HCl(aq) solution for the deposition of SRT/PSS multilayers on the base films was prepared by dissolving 20 mg of PSS in 10 mL of the 1 M NaCl/pH 3 HCl(aq) stock solution. A 1 mg/mL SRT deposition solution was prepared by suspending ∼60 mg of SRT solids in ∼60 mL of pH 3 HCl(aq) solution. The mixture was shaken for ∼5 min and then sonicated for 10 min to yield a solution. The PSS−SRT or PSS−rSRT multilayers were assembled on EDA-coated quartz substrates[45] using a dip-coating method. The quartz was submerged in the solution of PSS for 20 min before being washed three times for 2 min each in water. Afterward, the substrate was placed in the SRT (or rSRT) solution for 20 min and again washed. The enzyme-containing multilayer was created on cotton and glass surfaces. Initially, two bilayers of PSS−SRT were built on the substrates as described above to prevent inhibition of enzyme activity. A solution of 2 mg urease/mL pH 6.0 HCl(aq) was prepared by dissolving 10 mg of urease into 5 mL of pH 6.0 HCl(aq) solution. Atop of the PSS−SRT multilayers, bilayers of UE−SRT were created using the dip-coating method. The cloth or glass substrates were dipped coated into the urease containing solution for 20 min and then triple washed in DI water for 2 min. The substrate was then dipped in the solution of SRT (or rSRT) for 20 min and again washed in DI water. This process was repeated to build the desired number of UE−SRT bilayers.

Kinetics of Urease Enzyme. Kinetic data of the enzyme are extracted from the fluorescent intensity of the solutions monitored by the Tecan plate reader. To convert fluorescence intensity into a change in the pH of the solution, a calibration of fluorescence intensity against known pH values was determined. We determined the fluorescence intensity changes linearly in the 6.2−6.8 pH range at a rate of 2440 arb units/pH unit. Further, a change in pH of solution may be converted to a reaction rate by applying the Henderson−Hasselbalch equation. Since ammonia is a weak base, it may be ignored from the Henderson−Hasselbalch analysis. Further, the dye's contribution will also be ignored as its concentration is much lower than that of the phosphate buffer, pK_a 6.8. The Henderson−Hasselbalch equation applied to this system is displayed below where $[A^-]$ is the conjugate base. A direct calculation from pH value to reaction rate is obtained, where A^- (pH) is the concentration of the conjugate base at a specific pH.

$$[A^-]\,(\mathrm{pH}) = \frac{0.1 \times 10^{\mathrm{pH}-6.8}}{1 + 10^{\mathrm{pH}-6.8}}$$

For urease the concentration of reacted NH_3 is calculated using the reaction

$$NH_3 \text{ liberated} = \frac{1}{2}[A^-(6.2) - A^-(\mathrm{pH})]$$

The urease enzyme is rated at 50−100 units per mg solids, in which a micromolar unit is defined as liberating 1.0 μmol of NH_3 from urea per minute at pH 7.0 and at 25 °C. It is important to remember that one molecule of urea is hydrolyzed into two molecules of NH_3. In the case of the free enzyme we know 0.055 mg of urease was present during the reaction. From the linear region we note 1.67 μmol of NH_3 was liberated after 1 min. Using the known quantity of enzyme, 0.055 mg of urease solid, we can calculate the enzyme had an activity of 30.4 units per mg solid. This is close to the enzyme's rating of 50−100 units

DOI: 10.1021/acsami.6b05232
ACS Appl. Mater. Interfaces XXXX, XXX, XXX−XXX

per mg solid. We can use this calculated activity to estimate the amount of enzyme existing in the LbL films, which were deposited on a 4 × 4 cm^2 glass piece. In the five-bilayer UE/SRT film after 15 min 2.00 μmol of NH_3 was liberated. Using the ~30 units determined earlier, we calculated 4.42 μg of enzyme or 0.28 $\mu g/cm^2$, which was encapsulated in the SRT film. Similarly, in the five-bilayer UE/rSRT film 3.11 μmol of NH_3 was liberated after 15 min. Using the same calculation, we determined 6.90 μg of urease or 0.43 $\mu g/cm^2$ was encapsulated in rSRT film.

UV−Vis Absorbance. UV−vis absorbance spectra were acquired using a double-beam Varian Cary 5000 spectrophotometer. Solution spectra were taken using matched b = 1.00 cm path length quartz cuvettes and referenced against a water blank baseline. Spectra of multilayer films on quartz slides were referenced to an EDA-coated quartz slide baseline. The absorbance of multilayer films on quartz slides was determined for wavelength of 200−800 nm at steps of 1 nm. Spectra of 1−10 bilayers of SRT/PSS or rSRT/PSS were obtained. The absorbance of 9.5 SRT/PSS was also recorded to assess the contribution of the PSS to the absorbance.

ζ-Potential. ζ-Potential measurements were obtained with a Malvern Zetasizer ZS nano instrument. All calculations of zeta potential were produced by analyzing 100 scans each. Controlled pore glass beads 75−120 μm in diameter modified with EDA were used as the support for the multilayer structure. Prior to measurement, 10 mg of controlled pore glass (CPG) beads is filtered using vacuum filtration with a Buencher filter with 10−20 μm pores. These beads are resuspended in 1.3 mL of DI water adjusted to pH 6 in a 1.5 mL centrifuge tube. The beads were allowed to fall out of solution for 5 min, leaving a small portion suspended in solution. Afterward, 1 mL of solution was taken from the tube and transferred into the 1 mL cuvette for ζ-potential measurement. After measurement the beads are concentrated using the vacuum filtration and resuspended in 5 mL of appropriate polyion solution. The beads in polyion solution were stirred at 400 rpm for 30 min. Afterward, the beads were again separated from solution using a vacuum filtration method. After deposition of polyion the CPG beads were rinsed with DI water with three times to ensure unbound polyions are removed. The particles again were redispersed in deionized water for the next ζ-potential measurement.

Enzyme Kinetics. The activity of urease incorporated into the multilayered structure was performed by a colorimetric assay[19] using a fluorescent pH-sensitive dye hydroxypyrene-3,6,8-trisulfonic (HTPS) (Sigma-Aldrich, St. Louis, MO). A solution of 0.1 M phosphate(aq) was adjusted to pH 6.2 to ensure the pH change occurred within the linear region of the HTPS dye. This solution was used to create a solution containing 20 mM urea (Sigma-Aldrich, St. Louis, MO) and 2 mM HTPS. The pH-sensitive dye enzyme kinetics was monitored using a Tecan F200 PRO plate reader. The multilayered structure was formed on a 500 μm thick piece of borofloat glass using the procedure described above and placed into a 96-well plate. A 110 μL aliqot of the solution containing urea and HTPS was added to the well plate. This solution was monitored at 10 s intervals for 20 min using the plate reader. The excitation and emission filters on the plate reader were set to wavelengths of 460 and 510 nm, respectively. The signal obtained from the well with a glass piece containing 0 layers of urease was collected to correct for fluorescent quenching.

Textile Preparation. Merino wool (Supramerino 2/30, 7500 ypp, 9037-001), cotton (Ecocot, 7000 ypp, 4500-002), and linen (Linen 14, 7000 ypp, 9814-002) yarns were purchased from Silk City Fibers (Paterson, NJ) and were knitted into fabrics. The diameters of fibers were measured with a caliper (i.e., linen 0.3 mm, wool 0.4 mm, and cotton 0.5 mm). Samples of linen, cotton, and wool were prepared using 152 wales by 68 courses. Samples were knit on the Shima 122SSGSV machine, which has 12 needles per inch (12 gauge).

Mechanical Testing. Samples with desired dimensions were cut from the fabrics and used in the experiments. SRT-textile samples were dipped into a 50 mg/mL solution of native *Loligo vulgaris* SRT in 1,1,1,3,3,3-hexafluoro-2-propanol (HFIP) until soaked and were dried overnight at room temperature in a fume hood. Later, LbL layers were built on modified textile surface. SRT-wool healed samples were immersed in water at 70 °C and were compressed together with polydimethylsiloxane (PDMS) molds with a pressure of 1 MPa for 1 min. Mechanical testing of the textile samples was performed in a TA 800Q DMA instrument with film-tension clamps. Stress−strain curves were obtained at a constant strain rate of 5%/min and a preload of 0.01 N.

■ ASSOCIATED CONTENT

Ⓢ Supporting Information

The Supporting Information is available free of charge on the ACS Publications website at DOI: 10.1021/acsami.6b05232.

We demonstrated self-healing feature of multilayers constructed structural proteins by the method of polyelectrolyte layer-by-layer. The results presented in this video clearly show the self-healing feature of the multilayers and their improved mechanical properties compared to the conventional textiles such as cotton and wool (AVI)

■ AUTHOR INFORMATION

Corresponding Authors

*E-mail: walter.dressick@nrl.navy.mil (W.J.D.).
*E-mail: mdemirel@engr.psu.edu (M.C.D.).

Author Contributions

M.C.D. and W.D. conceived the idea, planned, and supervised the research. D.G. prepared the LbL films and measured the enzyme activity. A.P. performed the mechanical measurements. H.J. worked on the cloning, recombinant expression and purification of the squid protein. M.C.D., W.D., D.G., and G.D. contributed to writing and revising the manuscript. All authors agreed on the final content of the manuscript.

Notes

The authors declare no competing financial interest.

■ ACKNOWLEDGMENTS

M.C.D., A.P., and H.J. were supported by the Army Research Office under Grant W911NF-16-1-0019 and a seed grant of Materials Research Institute of the Pennsylvania State University. W.D. was supported by the Naval Research Laboratory through the internal 6.1 research program funded by the Office of Naval Research. S.T./D.G. and G.D. were supported by Pennsylvania State University and Drexel University, respectively.

■ REFERENCES

(1) Kessler, M. Self-healing: a new paradigm in materials design. *Proc. Inst. Mech. Eng., Part G* **2007**, *221* (4), 479−495.
(2) Syed, J. A.; Tang, S.; Lu, H.; Meng, X. Smart PDDA/PAA multilayer coatings with enhanced stimuli responsive self-healing and anti-corrosion ability. *Coll. Surf., A* **2015**, *476*, 48−56.
(3) Singh, A.; Lee, Y.; Dressick, W. J. Self-Cleaning Fabrics for Decontamination of Organophosphorous Pesticides and Related Chemical Agents. *Adv. Mater.* **2004**, *16* (23−24), 2112−2115.
(4) Lee, Y.; Stanish, I.; Rastogi, V.; Cheng, T.-c.; Singh, A. Sustained enzyme activity of organophosphorus hydrolase in polymer encased multilayer assemblies. *Langmuir* **2003**, *19* (4), 1330−1336.
(5) Hager, M. D.; Greil, P.; Leyens, C.; van der Zwaag, S.; Schubert, U. S. Self-Healing Materials. *Adv. Mater.* **2010**, *22* (47), 5424−5430.
(6) Decher, G. Fuzzy nanoassemblies: toward layered polymeric multicomposites. *Science* **1997**, *277* (5330), 1232−1237.
(7) Schaaf, P.; Voegel, J. C.; Jierry, L.; Boulmedais, F. Spray-Assisted Polyelectrolyte Multilayer Buildup: from Step-by-Step to Single-Step Polyelectrolyte Film Constructions. *Adv. Mater.* **2012**, *24* (8), 1001−1016.

DOI: 10.1021/acsami.6b05232
ACS Appl. Mater. Interfaces XXXX, XXX, XXX−XXX

(8) Krogman, K.; Zacharia, N.; Schroeder, S.; Hammond, P. Automated process for improved uniformity and versatility of layer-by-layer deposition. *Langmuir* **2007**, *23* (6), 3137−3141.
(9) Zhuk, A.; Sukhishvili, S. A. Stimuli-responsive layer-by-layer nanocomposites. *Soft Matter* **2013**, *9* (21), 5149−5154.
(10) Schmitt, J.; Decher, G.; Dressick, W. J.; Brandow, S. L.; Geer, R. E.; Shashidhar, R.; Calvert, J. M. Metal nanoparticle/polymer superlattice films: fabrication and control of layer structure. *Adv. Mater.* **1997**, *9* (1), 61−65.
(11) Bassim, N. D.; Dressick, W. J.; Fears, K. P.; Stroud, R. M.; Clark, T. D.; Petrovykh, D. Y. Layer-by-layer assembly of heterogeneous modular nanocomposites. *J. Phys. Chem. C* **2012**, *116* (2), 1694−1701.
(12) Dressick, W. J.; Soto, C. M.; Fontana, J.; Baker, C. C.; Myers, J. D.; Frantz, J. A.; Kim, W. Preparation and Layer-by-Layer Solution Deposition of Cu(In, Ga)O_2 Nanoparticles with Conversion to Cu(In, Ga)S_2 Films. *PLoS One* **2014**, *9* (6), e100203.
(13) Richert, L.; Lavalle, P.; Payan, E.; Shu, X. Z.; Prestwich, G. D.; Stoltz, J.-F.; Schaaf, P.; Voegel, J.-C.; Picart, C. Layer by layer buildup of polysaccharide films: physical chemistry and cellular adhesion aspects. *Langmuir* **2004**, *20* (2), 448−458.
(14) Saydjari, A.; Long, J. P.; Dressick, W. J.; Simpkins, B. S. Optical interference effect corrections for absorbance spectra of layer-by-layer thin films bearing covalently bound dye. *Chem. Phys. Lett.* **2014**, *608*, 328−333.
(15) Kharlampieva, E.; Kozlovskaya, V.; Zavgorodnya, O.; Lilly, G. D.; Kotov, N. A.; Tsukruk, V. V. pH-responsive photoluminescent LbL hydrogels with confined quantum dots. *Soft Matter* **2010**, *6* (4), 800−807.
(16) Richardson, J. J.; Björnmalm, M.; Caruso, F. Technology-driven layer-by-layer assembly of nanofilms. *Science* **2015**, *348* (6233), aaa2491.
(17) Dressick, W. J.; Wahl, K. J.; Bassim, N. D.; Stroud, R. M.; Petrovykh, D. Y. Divalent−anion salt effects in polyelectrolyte multilayer depositions. *Langmuir* **2012**, *28* (45), 15831−15843.
(18) Jiang, G.; Baba, A.; Advincula, R. Nanopatterning and fabrication of memory devices from layer-by-layer poly (3, 4-ethylenedioxythiophene)-poly (styrene sulfonate) ultrathin films. *Langmuir* **2007**, *23* (2), 817−825.
(19) Gaddes, D. E.; Demirel, M. C.; Reeves, W. B.; Tadigadapa, S. Remote calorimetric detection of urea via flow injection analysis. *Analyst* **2015**, *140* (23), 8033−8040.
(20) Wood, K. C.; Boedicker, J. Q.; Lynn, D. M.; Hammond, P. T. Tunable drug release from hydrolytically degradable layer-by-layer thin films. *Langmuir* **2005**, *21* (4), 1603−1609.
(21) Yuan, J.; Wang, Z.; Zhang, Y.; Shen, Y.; Han, D.; Zhang, Q.; Xu, X.; Niu, L. Electrostatic layer-by-layer a of platinum-loaded multiwall carbon nanotube multilayer: A tunable catalyst film for anodic methanol oxidation. *Thin Solid Films* **2008**, *516* (18), 6531−6535.
(22) Porcel, C.; Lavalle, P.; Decher, G.; Senger, B.; Voegel, J.-C.; Schaaf, P. Influence of the polyelectrolyte molecular weight on exponentially growing multilayer films in the linear regime. *Langmuir* **2007**, *23* (4), 1898−1904.
(23) Schönhoff, M.; Ball, V.; Bausch, A. R.; Dejugnat, C.; Delorme, N.; Glinel, K.; von Klitzing, R.; Steitz, R. Hydration and internal properties of polyelectrolyte multilayers. *Coll. Surf., A* **2007**, *303* (1), 14−29.
(24) Bai, S.; Sun, C.; Yan, H.; Sun, X.; Zhang, H.; Luo, L.; Lei, X.; Wan, P.; Chen, X. Healable, Transparent, Room-Temperature Electronic Sensors Based on Carbon Nanotube Network-Coated Polyelectrolyte Multilayers. *Small* **2015**, *11* (43), 5807−5813.
(25) Hu, X.; Xu, S.; Feng, S.; Wang, J.; Xu, J. Saline-enabled self-healing of polyelectrolyte multilayer films. *RSC Adv.* **2015**, *5* (12), 8877−8881.
(26) Wang, X.; Liu, F.; Zheng, X.; Sun, J. Water-Enabled Self-Healing of Polyelectrolyte Multilayer Coatings. *Angew. Chem., Int. Ed.* **2011**, *50* (48), 11378−11381.
(27) Wang, X.; Wang, Y.; Bi, S.; Wang, Y.; Chen, X.; Qiu, L.; Sun, J. Optically transparent antibacterial films capable of healing multiple scratches. *Adv. Funct. Mater.* **2014**, *24* (3), 403−411.
(28) Chen, X. C.; Ren, K. F.; Zhang, J. H.; Li, D. D.; Zhao, E.; Zhao, Z. J.; Xu, Z. K.; Ji, J. Humidity-Triggered Self-Healing of Microporous Polyelectrolyte Multilayer Coatings for Hydrophobic Drug Delivery. *Adv. Funct. Mater.* **2015**, *25* (48), 7470−7477.
(29) Huang, X.; Bolen, M. J.; Zacharia, N. S. Silver nanoparticle aided self-healing of polyelectrolyte multilayers. *Phys. Chem. Chem. Phys.* **2014**, *16* (22), 10267−10273.
(30) Zhu, Y.; Yao, C.; Ren, J.; Liu, C.; Ge, L. Graphene improved electrochemical property in self-healing multilayer polyelectrolyte film. *Coll. Surf., A* **2015**, *465*, 26−31.
(31) Zhu, Y.; Yin, T.; Liu, C.; Fu, D.; Ge, L. Self-healing Polyelectrolyte Multilayer Composite Film with Microcapsules. *RSC Adv.* **2016**, *6* (15), 12100−12106.
(32) Skorb, E. V.; Andreeva, D. V. Layer-by-Layer approaches for formation of smart self-healing materials. *Polym. Chem.* **2013**, *4* (18), 4834−4845.
(33) Park, C. W.; South, A. B.; Hu, X.; Verdes, C.; Kim, J.-D.; Lyon, L. A. Gold nanoparticles reinforce self-healing microgel multilayers. *Coll. Polym. Sci.* **2011**, *289* (5−6), 583−590.
(34) Chen, D.; Wu, M.; Li, B.; Ren, K.; Cheng, Z.; Ji, J.; Li, Y.; Sun, J. Layer-by-Layer-Assembled Healable Antifouling Films. *Adv. Mater.* **2015**, *27* (39), 5882−5888.
(35) Zhu, Y.; Xuan, H.; Ren, J.; Ge, L. Self-healing multilayer polyelectrolyte composite film with chitosan and poly (acrylic acid). *Soft Matter* **2015**, *11* (43), 8452−8459.
(36) Demirel, M. C.; Cetinkaya, M.; Pena-Francesch, A.; Jung, H. Recent Advances in Nanoscale Bioinspired Materials. *Macromol. Biosci.* **2015**, *15* (3), 300−311.
(37) Pena-Francesch, A.; Akgun, B.; Miserez, A.; Zhu, W.; Gao, H.; Demirel, M. C. Pressure Sensitive Adhesion of an Elastomeric Protein Complex Extracted From Squid Ring Teeth. *Adv. Funct. Mater.* **2014**, *24* (39), 6227−6233.
(38) Pena-Francesch, A.; Florez, S.; Jung, H.; Sebastian, A.; Albert, I.; Curtis, W.; Demirel, M. C. Materials Fabrication From Native and Recombinant Thermoplastic Squid Proteins. *Adv. Funct. Mater.* **2014**, *24* (47), 7393−7401.
(39) Sariola, V.; Pena-Francesch, A.; Jung, H.; Çetinkaya, M.; Pacheco, C.; Sitti, M.; Demirel, M. C. Segmented molecular design of self-healing proteinaceous materials. *Sci. Rep.* **2015**, *5*, 13482.
(40) Bellomo, R.; Kellum, J. A.; Ronco, C. Acute kidney injury. *Lancet* **2012**, *380* (9843), 756−766.
(41) Lakard, B.; Herlem, G.; Lakard, S.; Antoniou, A.; Fahys, B. Urea potentiometric biosensor based on modified electrodes with urease immobilized on polyethylenimine films. *Biosens. Bioelectron.* **2004**, *19* (12), 1641−1647.
(42) Wang, H.; Malvadkar, N.; Koytek, S.; Bylander, J.; Reeves, W. B.; Demirel, M. C. Quantitative analysis of creatinine in urine by metalized nanostructured parylene. *J. Biomed. Opt.* **2010**, *15* (2), 027004.
(43) Liang, Z.; Wang, C.; Tong, Z.; Ye, W.; Ye, S. Bio-catalytic nanoparticles with urease immobilized in multilayer assembled through layer-by-layer technique. *React. Funct. Polym.* **2005**, *63* (1), 85−94.
(44) Sakr, O. S.; Borchard, G. Encapsulation of enzymes in Layer-by-Layer (LbL) structures: latest advances and applications. *Biomacromolecules* **2013**, *14* (7), 2117−2135.
(45) Dressick, W. J.; Kondracki, L. M.; Chen, M.-S.; Brandow, S. L.; Matijević, E.; Calvert, J. M. Characterization of a colloidal Pd (II)-based catalyst dispersion for electroless metal deposition. *Coll. Surf., A* **1996**, *108* (1), 101−111.
(46) Nestler, P.; Paßvogel, M.; Helm, C. A. Influence of Polymer Molecular Weight on the Parabolic and Linear Growth Regime of PDADMAC/PSS Multilayers. *Macromolecules* **2013**, *46* (14), 5622−5629.
(47) Daniels, G. A.; Petrovich, P. A. Conformable self-healing ballistic armor. US Patent 7,966,923, 2012.

DOI: 10.1021/acsami.6b05232
ACS Appl. Mater. Interfaces XXXX, XXX, XXX−XXX